LATTICE-BOLTZMANN STUDY OF THE WIND-DRIVEN DYNAMICS OF SHALLOW SEA WATER

EMPLEO DEL MÉTODO DE LATTICE BOLTZMANN EN EL ESTUDIO DE LA DINÁMICA DE LAS AGUAS COSTERAS COMO CONSECUENCIA DEL ARRASTRE DEL VIENTO

R. Martin-Barrios†, A. Martínez-Mesa, L. Uranga-Piña

DynAMoS (Dynamical processes in Atomic and Molecular Systems), Faculty of Physics, University of Havana, 10400 Havana, Cuba; rmartin@fisica.uh.cu†
† corresponding author

Recibido 20/3/2017; Aceptado 5/9/2017

The Lattice-Boltzmann method is a powerful tool to simulate fluid dynamics in complex geometries. In this work, this algorithm is applied to the modeling of wind-driven flow of shallow sea water in interaction with the shore and the seabed. The macroscopic fluid properties (velocities, pressure) are computed as moments of the particle distribution functions. The present two-dimensional implementation allows to investigate the influence, on the equilibrium velocity-field of the sea, of the various parameters determining the topography of the shore for two different coastal models. The effect of the variations of the average density and pressure of the liquid, and the wind velocity on the steady flow under the surface of the sea is also addressed.

El método de Lattice-Boltzmann constituye una poderosa herramienta para simular la dinámica de fluidos confinados en regiones con geometría compleja. En este trabajo, este algoritmo se aplica a la modelación del flujo de las aguas costeras como consecuencia del arrastre del viento, en interacción con la costa y el fondo marino. Las propiedades macroscópicas del fluido (velocidad, presión) se calculan a partir de los momentos de las funciones de distribución. El esquema bidimensional implementado permite investigar la influencia, sobre el campo de velocidades del fluido en equilibrio, de la topografía del litoral para dos modelos distintos del perfil de la costa. También se estudian los efectos de las variaciones de la densidad y la presión del líquido y de la velocidad del viento sobre el flujo estacionario bajo la superficie del mar.

PACS: Dynamics of the upper ocean, 92.10.Fj; Beach, coastal, and shelf processes, 91.50.Cw; Lattice theory and statistics, 05.50.+q

I. INTRODUCTION

Despite the progress made during the last decades in the study of ocean dynamics, the quantification and prediction of these processes remains a challenging task [1]. The ocean is a turbulent and stratified fluid displaying various phenomena occurring in very different space and time scales.

Physical modelling constitutes a key ingredient in the analysis of hydrodynamic processes in the coastal region. The theoretical investigation of the main phenomena in coastal waters is often divided in two phases. First, mathematical and numerical models are built to account for the main characteristics of the relevant hydrodynamical processes. In a second stage, these hydrodynamic models serve as a basis for other studies regarding, for instance, the sediment transport, surface waves and water quality.

The dynamical processes in the nearshore region (e.g., coastal currents, tides, surface waves, tsunamis) are usually determined by external driving forces. For practical purposes, many investigations on the sea water dynamics close to the coast neglect the effect of the liquid-air interface. In these studies, the motion of the fluid is described in terms of parameters such as the Iribarren number, which characterizes the breaking of sea waves and its dependence on the water depth, the profile of the coast, etc. [2] .

The chief difference between coastal and deep ocean waters is the influence, on the fluid motion, of the physical constraints imposed by the sea bottom (at relatively shallow depths) and the coastline. From the numerical modelling perspective, the irregular nature of coastal profiles translates in complex boundary conditions to be imposed to the solutions of the Navier-Stokes equation, thereby hindering the theoretical description of the associated phenomena.

The Lattice-Boltzmann method (LBM) provides a computational alternative to the solution of the Navier-Stokes equation, which is well suited to incorporate the interaction of the fluid with boundaries of arbitrary shape (such as the coastline, wharfs, ships) [3,4]. The LBM is based on the discretization of the Boltzmann transport equation, which governs the time evolution of microscopic probability distribution functions in the fluid. The discretization yields a numerical method for evaluating the corresponding macroscopic distribution functions on a Cartesian mesh. Extensive theoretical and numerical evidence have been provided which supports the convergence of the LBM towards the solution of the Navier-Stokes equation [5]. Moreover, both the continuity equation and the Navier Stokes equation can be obtained from the latter LBM via a Chapman-Enskog expansion [6]. Beyond applications to the modelling of ocean dynamics, the LBM has been used to simulate many problems in magnetohydrodynamics, turbulence, colloidal suspensions, multiphase flow, etc. [3,7].

In this work, the LBM is applied to the investigation of the wind-driven circulation of shallow sea water. We assess the influence of the velocity of the wind dragging the upper surface of the fluid on the equilibrium velocity field, and the dependence of the latter on the shape of the coast.

Although there are various applications of the Lattice-Boltzmann technique to the study of the coastal hydrodynamics [8–11], these studies focus on the solution of the so-called shallow water equations, which can be obtained from the Navier-Stokes equations by integrating the dependence of the fluid fields on the water depth. The present implementation extends the applicability of the LBM to the description of the fluid density and velocity fields beyond the approximations inherent to the shallow water equations (the latter are valid if the horizontal length-scale is much larger than the vertical length-scale, the vertical velocity of the fluid is small, etc.), thereby providing a more realistic description of hydrodynamical phenomena near the shore.

In the following, we describe the two-dimensional implementation of the Lattice-Boltzmann method, the coastal profiles and the boundary conditions used in the calculations. Some numerical examples of the application of the LBM to the simulation of the nearshore dynamics are presented in the section results. Finally, some conclusions are drawn.

II. METHODOLOGY

II.1. Lattice-Boltzmann Method

For an isolated system composed by identical particles undergoing two-body uncorrelated collisions, the time evolution of the single-particle phase-space distribution function $f(\vec{x},t)$ is governed by the Boltzmann transport equation:

$$\frac{\partial f}{\partial t} + \vec{u}\cdot\nabla f = \Omega, \tag{1}$$

where $\vec{x}$ and $\vec{u}$ stand for positions and velocities of the particles, and Ω is the collision operator.

The LBM simplifies the description of gas dynamics underlying the Boltzmann equation (1) by reducing the number of fluid particles and fixing their positions at the nodes of a lattice [3, 5]. In the present paper, where the motion of the fluid occurs in two dimensional space, the Lattice-Boltzmann particles are restricted to stream in 9 possible directions, including the possibility to stay at rest, as represented in Figure 1. These set of directions of motion are called the microscopic velocities, and they will be denoted by the vectors $\vec{e_i}$ where $i = 0, ..., 8$. This two-dimensional model is commonly known as the D2Q9 model [3].

Likewise, a discrete probability distribution function $f_i(\vec{x},t), i = 0.., 8$, (which describes the probability of streaming along each specific direction) is associated to each lattice site. The macroscopic density of the fluid can be obtained by summing over the components of the microscopic particle distribution function:

$$\rho(\vec{x},t) = \sum_{i=0,8} f_i(\vec{x},t). \tag{2}$$

Furthermore, the macroscopic velocity $\vec{u}(\vec{x},t)$ is computed as the average of the microscopic velocities $\vec{e_i}$ weighted by the distribution functions f_i:

$$\vec{u}(\vec{x},t) = \frac{1}{\rho}\sum_{i=0,8} c f_i(\vec{x},t)\vec{e_i}, \tag{3}$$

where $c = \frac{\Delta x}{\Delta t}$ is the so-called lattice speed.

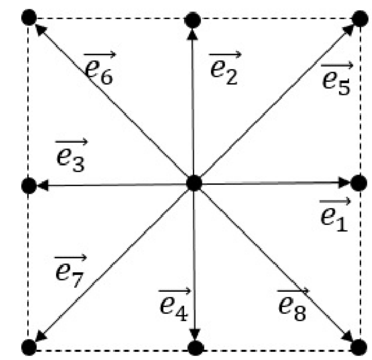

Figure 1. Velocity vectors corresponding to one lattice node in the D2Q9 model.

Diffusive and collision contributions to the variation of the microscopic distribution function are taken into account separately in the LBM. Therefore, the methodology comprises two key steps: streaming and collision, which are computed separately.

In Figure 2, it is shown schematically how the streaming step takes place for the interior nodes. At each point in the lattice, the values of the discrete distribution function along the different directions are passed to the neighbouring nodes. This prescription applies for the inner nodes only, the treatment of the points lying on the edges of the grid will be described in the following subsection.

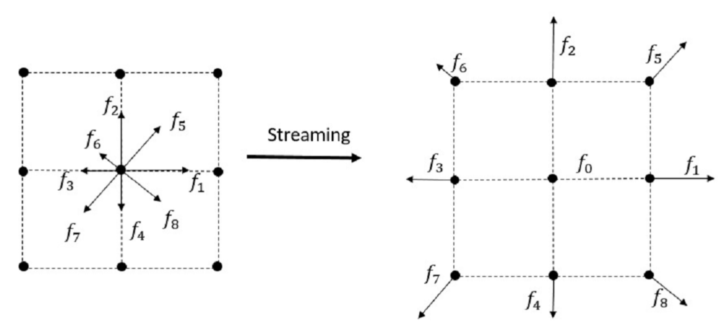

Figure 2. Schematic representation of the streaming process in the LBM at an interior lattice node.

Employing the Bhatnagar-Gross-Krook approximation for the collision operator, the corresponding process can be modelled through the equation:

$$f_i(\vec{x} + c\vec{e_i}\Delta t, t + \Delta t) - f_i(\vec{x},t) = -\frac{f_i(\vec{x},t) - f_i^{eq}(\vec{x},t)}{\tau}. \tag{4}$$

In equation (4), the function f_i^{eq} represents the phase-space distribution of the fluid in equilibrium. The parameter τ is the relaxation time towards local equilibrium, and is related to the kinematic viscosity ν via the expression:

$$\nu = \frac{2\tau - \Delta t}{6}\left(\frac{\Delta x}{\Delta t}\right)^2 . \qquad (5)$$

The calculations were performed using our own implementation of the LBM, which was written in Fortran 95. The present implementation was benchmarked against the numerical solutions of model problems [12], showing a similar accuracy. The propagation stops when the relative variation of the velocity field at every lattice point is lower than 10^{-4}. All the simulations performed were found to converge to the stationary distribution after about 10^5 iterations. Typically, the CPU running time (for calculations employing 400×200 grid points) was approximately 3 hours in a personal computer (ASUS, model X4535A, Dual Core processor at 1.60 GHz). Since the update of the phase space distribution function at the lattice points is a local process, the computational cost of the LBM is expected to grow linearly with the number of nodes. However, the algorithm is easily parallelizable, and the calculation time can be significantly reduced, for example, by using graphical processors [13].

II.2. Boundary conditions

Three different types of boundaries need to be modelled in the present study, namely the sea-air interface, the incoming velocity distribution of the fluid approaching the coast and the sea-soil interface. The corresponding boundary conditions are chosen as follows:

(i) In order to mimic the influence of the dragging force of the wind on the upper layer of the sea water, a constant velocity u_{top} was set for these mesh points. The value of u_{top} is chosen according to the empirical relation $u_{top} = 0.03\ u_{wind}$, which holds for steady wind velocities between 5 and 30 m·s^{-1} [14]. u_{wind} denotes the velocity at 10 meters height from the surface of the ocean.

(ii) Assuming a laminar flow, and that no forces other than wind and viscous stresses act on the fluid layers in the horizontal direction, a constant velocity gradient

$$\frac{\Delta u}{\Delta z} = \frac{\sigma}{\rho_{sea}\nu} \qquad (6)$$

is established for the horizontal velocity of deep ocean waters (i.e., at distances from the coast for which the fluid interaction with the seabed can be neglected). In equation (6), ν and ρ_{sea} represent the kinematic viscosity and density of the water, respectively, and σ is the wind stress. Furthermore, the stress σ is related to the velocity of wind by the empirical formula $\sigma = \rho_{air} C_d u_{wind}^2$ [14], where ρ_{air} is the density of the air and C_d is the drag coefficient.

With these ingredients we set the fluid velocities for the left-most grid points, assuming the following values for the parameters: ρ_{air} = 1.22 kg·m^{-3}, $C_d = 1.69 \cdot 10^{-3}$. It depends also on the density and on the kinematic viscosity of the sea water, for which several values were considered (see next section).

(iii) We consider the interaction of the moving fluid with two shore models: a step-like profile:

$$110\left[1 + \tanh\{\alpha(x - 250)\}\right] + 1, \qquad (7)$$

and the so-called Dean profile [15]:

$$A(400 - x)^{\frac{2}{3}} + 200. \qquad (8)$$

These two models allow to characterize the fluid dynamics in present of sharp and smooth variations of the water depth near the coast. Moreover, the modification of the parameters α and A allow to tune the length-scale of these variations for both profiles in a continuous way.

The collisions of fluid particles with the solid-fluid boundary are assumed to be elastic. To reflect this behaviour, the distribution functions are reversed at every time step for the grid points on the solid-liquid interface.

The relations arising from imposing constant velocities at the edge points (conditions (i) and (ii)) and the choice (iii) are known as Zou-He and bounce-back boundary conditions, respectively [16].

III. RESULTS

We performed calculations of the wind-driven ocean circulation using the LBM and employing the Maxwell-Boltzmann distribution as the equilibrium distribution function. All the relevant parameters (velocity of the wind, average density and pressure of the water, α and A) were systematically varied. As an illustration, in this section we present some results computed assuming u_{wind} = 5 m·s^{-1}, Δz = 0.01 m, $\tau = 0.8$, ρ_{sea} = 1025 kg·m^{-3} and $\nu = 10^{-6}$ m^2·s^{-1}. The latter two values correspond to the density and the kinematic viscosity of water at a temperature of 293 K.

In Figure 3, we show the equilibrium velocity field established in the nearshore region for the hyperbolic tangent model and for two different values of the parameter α. It can be seen, that in both cases there is a strong influence of the water-soil interface in the circulation pattern leading to vortex formation. Moving away from the centre of the vortex, the fluid velocity initially increases, but this behaviour is replaced by a reduction of the current as we approach the sea bottom. The fluid is at rest in the region close to the fluid-solid boundary, and this area is broader for the more abrupt coast profile.

Since $\nabla \times \vec{u}$ represents twice the rotational velocity of the fluid, the right panels of Figure 3 indicate that vortex rotation is faster for the water interacting with the smoother profile, while the portion of the fluid having non-vanishing rotational velocities is smaller in this case. On the other hand, there is a region of positive values of the rotor field, which can be attributed to velocity gradients rather to the presence of vortices.

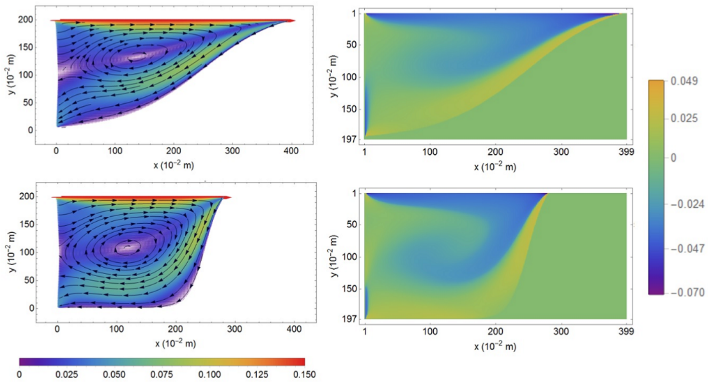

Figure 3. Velocity field (left panels, in m/s) and its rotor (right panels) of the fluid interacting with the coast following an hyperbolic tangent profile. The spatial variation of the coast model is characterized by the parameters $\alpha = 0.0075$ (top) and $\alpha = 0.035$ (bottom).

For the Dean profile, a more complex pattern of fluid velocities is observed. It includes a zero-velocity fringe in the fluid connecting to different centres around which the fluid rotates. The results in this case resemble those obtained for the slowly varying hyperbolic tangent profile, which suggests that the wind-driven coastal dynamics is determined in first place by the overall slope of the sea-shore boundary instead of the details of the topography of the coast.

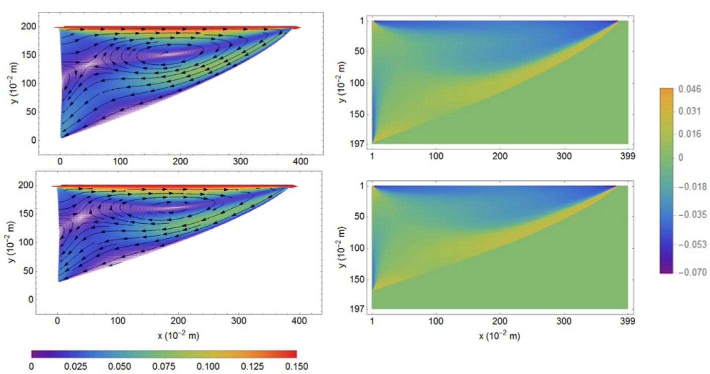

Figure 4. Velocity field (left panels, in m/s) and its rotor (right panels) of the fluid interacting with the coast following a Dean profile. The spatial variation of the coast model is characterized by the parameters $A = -4$ (top) and $A = -3.5$ (bottom).

IV. CONCLUSIONS

As a contribution to the development and application of ocean models for coastal applications, we simulated the dynamics of wind-driven shallow sea water with the Lattice-Boltzmann method. The numerical efficiency of this implementation allowed to investigate the effects of the interaction of the ocean with the coast for different values of the parameters (wind velocity, average density and pressure of the liquid) spanning the complete range of interest in practical situations. The solution of the Lattice-Boltzmann equations on a two-dimensional grid withouth performing the standard depth-averaging, allows to extend the applicability of the LBM to the description of the coastal hydrodynamics beyond the approximations inherent to the shallow water equations. The results reported in the previous section show that vertical currents and their dependence on the water depth play a significant role in the determination of undertow patterns. Therefore, their accurate theoretical description is important to achieve a better understanding of coastal phenomena.

The results of the present numerical scheme can be directly combined with existing models to predict the dynamics of coast sediments, concentration of nutrients, etc. [17] . For example, the circulation pattern observed near the coast, in particular the dependence of the rotational velocity on the slope of the coast profile, is expected to play a major role in phenomena like sediment transport.

REFERENCES

[1] K. W. Chau, "Modelling for coastal hydraulics and engineering", 1st Ed. (Taylor and Francis, London, 2010).

[2] M. Sukop, D. T. Thorne, "Lattice Boltzmann modeling: an introduction for geoscientists and engineers", 1st Ed. (Springer Verlag, London, 2006).

[3] S. Succi, "The Lattice Boltzmann equation for fluid dynamics and beyond", 1st Ed. (Oxford University Press, UK, 2001).

[4] J. M. Buick, C. A. Greated, Phys. Rev. E **61**, 5307 (2000).

[5] Z. Guo, B. Shi, N. Wang, J. Comput. Phys. **165**, 288 (2000).

[6] S. Chapman, T. Cowling, "The mathematical theory of nonuniform gases", 1st Ed. (Cambridge University Press, UK, 1970).

[7] A. A. Mohamad, "Lattices Boltzmann Method Fundamentals and engineering applications with computers code", 3rd Ed. (Springer-Verlag, London, 2011).

[8] J. G. Zhou, "Lattice Boltzmann methods for shallow water flows", 2nd Ed. (Springer-Verlag, London, 2004).

[9] H. Liu, J. G. Zhou, R. Burrows, Adv. Water Resour. **33**, 387 (2010).

[10] J. G. Zhou, H. Liu, Phys. Rev. E **88**, 023302 (2013).

[11] Y. Zhang, L. Li, D. V. Erler, I. Santos, D. Lockington, Hydrol. Processes **31**, 2530 (2017).

[12] S. Chen, G. D. Doolen, Annu. Rev. Fluid Mech. **30**, 329 (1998).

[13] C. Obrecht, F. Kuznik, B. Tourancheau, J.-J. Roux, Comput. Math. Appl. **65**, 252 (2013).

[14] J. E. Weber, J. Phys. Oceanography **13**, 524 (1982).

[15] R. G. Dean, J. Coastal Res. **7**, 53 (1991).

[16] Q. Zou, X. He, J. Phys. Fluids **8**, 2527 (1997).

[17] N. Grunnet, S. Lohier, R. Deigaard, I. Broker, M. Huiban, Littoral 2008: 9th International conference, Venice (2008).